Diamond turning of high-precision roll-to-roll imprinting molds for fabricating subwavelength gratings

Chun-Wei Liu,[a] Jiwang Yan,[b] and Shih-Chieh Lin[c,*]
[a]Industrial Technology Research Institute, Mechanical and Systems Research Laboratories, 195, Section 4, Chung Hsing Road, Chutung, Hsinchu 310, Taiwan
[b]Keio University, Department of Mechanical Engineering, Hiyoshi 3-14-1, Kohoku-ku, Yokohama 223-8522, Japan
[c]National Tsing Hua University, Department of Power Mechanical Engineering, 101, Section 2, Kuang-Fu Road, Hsinchu 30013, Taiwan

Abstract. Diamond turning of high-precision molds is a vital process for the roll-to-roll-based ultraviolet resin imprinting process in fabricating subwavelength gratings. The effects of the grating shape and grating period on diffraction efficiencies and diffraction angles were simulated. Experiments were then conducted to examine the effects of shape design, grating period, and cutting speed on machinability of the mold. According to the optical measurement results, the performance of the subwavelength gratings matched the design well at various incident angles. The results confirm that diamond turning of high-precision molds is a feasible approach for ensuring the continual mass production of subwavelength gratings. [DOI: 10.1117/1.OE.55.6.064105]

Keywords: diffraction grating; subwavelength grating; optical design and fabrication; diamond machining; roll-to-roll ultraviolet embossing process.

Paper 151597 received Nov. 17, 2015; accepted for publication May 20, 2016; published online Jun. 8, 2016.

1 Introduction

Subwavelength structures are increasingly in demand for various applications, such as optoelectronics, biomedical components, environmental technology, and communications. Various techniques such as etching, lithography electroforming, excimer laser ablation, E-beam lithography, and the self-assembled technique have been used for forming components with subwavelength features.[1–13]

However, these methods are not cost-effective and are restricted to the processing of planar master tools with dimensional size. Roll-to-roll imprinting processes based on single-point diamond-turned molds are a competitive solution for the large-scale and cost-effective production of nanostructured components[14–16] and in particular roll-to-roll devices.[17]

Jones et al.[18] presented a focused-ion-beam fabricated diamond tool for producing submicron structures through a roll-based mastering method. Burr formation was minimized and the surface quality of the product was improved by optimizing the cutting tool's shape design and the microcutting process conditions. Hocheng and Hsieh[19] also used a diamond tool in machining an electroless plated-nickel layer to form a submicron-patterned prismatic mold. A sunlight guide panel/film was then formed by imprinting prismatic microstructures on a transparent substrate through ultraviolet (UV) imprinting and a roll-to-roll process.[20]

Zhang and Kun[21] suggested that when adopting the processing, structural, and physical parameters of the conventional forming for microforming, the influence of the size effects must be taken into account. Ikawa et al.[22] found that the sharper the microcutting edge, the smaller the minimum thickness of cutting. The uniformity of the work material and the affinity between the tool and the work material are also important factors for microcutting thickness. Drescher and Dow[23] displayed that the cutting forces generally followed expected trends, but at a small depth of cut, the force was higher than expected in general. Sawada et al.[24] experimentally showed that the cutting speed is the key component to manufacture the high-accuracy microgroove grating without any burr formation.

The current study investigated the feasibility of employing diamond turning in high-precision roll-to-roll imprinting molds for fabricating subwavelength gratings. First, the commercial software G-solver, which is based on a rigorous coupled wave analysis,[25,26] was used to study the effects of grating shapes and grating periods on the diffraction efficiencies (DEs) and diffraction angles; this examination was conducted to ensure that gratings with high efficiency were designed. Subsequently, experiments were then conducted to study the effects of cutting parameters on the quality of machined molds to guarantee the quality of subwavelength grating.

2 Optical Performance of Subwavelength Grating

Similar to designs in Refs. 27–30, subwavelength gratings were designed in the current study to effectively out-couple one of the primary colors ($\lambda_R = 650$ nm, $\lambda_G = 520$ nm, and $\lambda_B = 473$ nm) vertically through a light guide. The relationship between the diffraction angle and incident angle can be derived from the following grating equation:

$$m\lambda = \Lambda(n_2 \sin \theta_{dif} - n_1 \sin \theta_{inc}), \quad (1)$$

where Λ is the grating period, θ_{inc} is the incident angle, θ_{dif} is the diffraction angle, n_1 is the refractive index of the incident medium polymethyl methacrylate, n_2 is the refractive index

*Address all correspondence to: Shih-Chieh Lin, E-mail: sclin@pme.nthu.edu.tw

0091-3286/2016/$25.00 © 2016 SPIE

Table 1 Parameters of simulation.

Parameter	Levels
Tool vertex angle	90 deg
Lead side angle	15 deg, 30 deg, 45 deg, 60 deg, and 75 deg
Grating period	320, 400, and 500 nm
Wavelength	473, 532, and 621 nm
Incident angle	80.20 deg, 62.46 deg, and 60.7 deg

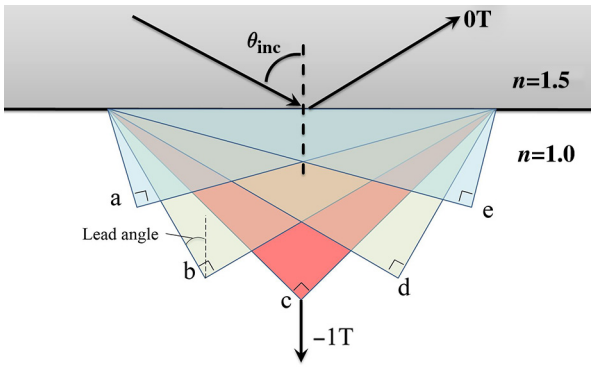

Fig. 1 V shapes with various lead side angles.

of air, and m is the diffraction order. The incident angle θ_{inc} was determined such that its diffraction angle of the first order for a certain primary color, θ_{dif}, was 0 deg. The DE, which is a function of the grating shape, grating period, and grating refractive index, as well as the first-order transmission efficiency (−1T) of the optical element should be sufficiently high. G-solver was adopted to study the effects of the grating design on the DE. Table 1 lists the parameters and levels used in these simulations. Figure 1 shows various tool geometries for these tests.

Table 2 shows the DE derived from simulations involving the vertical out-coupling of the primary colors. The corresponding incident angles θ_{inc} were derived using Eq. (1): 80.20 deg for blue light (473 nm) vertically out-coupled from a grating with a period of 320 nm, 62.46 deg for green light (532 nm) vertically out-coupled from a grating with a period of 400 nm, and 60.7 deg for red light (621 nm) vertically out-coupled from grating with a period of 500 nm. These results revealed that the diffraction coefficient was based on the grating shape, attracted color, and grating period. In general, a higher aspect ratio indicates a higher DE. However, the results of this study showed that the effects of the lead angle, grating period, and primary colors on efficiency varied significantly when an asymmetric shape was used. The results also revealed that the DE was higher when the light was incident from a gentle side (such as cases d and e) compared with when the light was incident from a steep side (such as cases a and b). Therefore, design with a large lead side angle (45 deg, 60 deg, and 75 deg) is preferred to ensure high efficiency.

Table 2 Effects of design parameters on DE according to vertically out-coupled primary colors.

	Red light source	Green light source	Blue light source
Grating shape	DE(−1T) (%)	DE(−1T) (%)	DE(−1T) (%)
(a) Grating period: 320 nm with θ_{inc} of 80.2 deg			
A	0.23	0.24	0.28
B	0.75	0.78	0.81
C	1.27	1.45	1.46
D	1.09	1.46	1.67
e	0.32	0.48	0.5
(b) Grating period: 400 nm with θ_{inc} of 62.46 deg			
a	0.72	0.93	1.15
b	2.33	2.74	3.51
c	4.38	4.74	5.66
d	4.31	5.27	5.87
e	1.36	1.98	2.43
(c) Grating period: 500 nm with θ_{inc} of 60.7 deg			
a	1.04	1.43	1.67
b	3.08	4.25	4.53
c	5.30	7.76	8.80
d	5.88	8.46	10.60
e	2.21	3.45	4.62

3 Experiments for Mold Machinability

Figure 2 shows a schematic of a diamond cutting tool. This study examined the effects of tool shape, grating period, and machine speed on the machinability of the molds used for processing the gratings. The levels of grating period were 320, 400, and 500 nm, the levels of turning speed were 63, 157, and 251 m/min, and the levels of lead side angle were 45, 60, and 75 deg. A fractional factorial design of 3^{3-1} was used for experiment planning. Table 3 shows the arrangement of the experimental conditions.

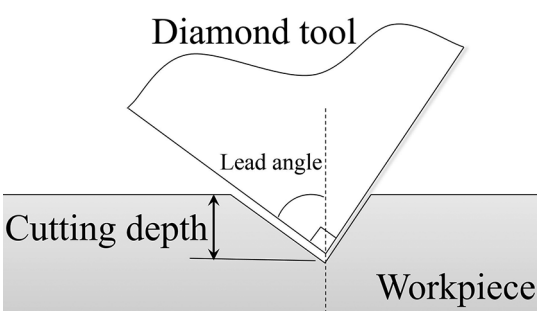

Fig. 2 Schematic of a diamond cutting tool.

Table 3 Experimental conditions.

Grating period (nm)	Roller speed (m/min)	Lead side angle (deg)
320	63	45
320	157	60
320	251	75
400	63	60
400	157	75
400	251	45
500	63	75
500	157	45
500	251	60

Figure 3(a) shows the diamond tool used to machine the mold, and Fig. 3(b) shows the lathe used to machine the mold on a drum roller. Figure 4 shows several molds with various periods and shapes mechanically grooved by diamond turning on a hard-copper roller with a diameter of 200 mm.

Figure 5 shows a scanning electron microscope (SEM) image of the diamond tool before and after machining.

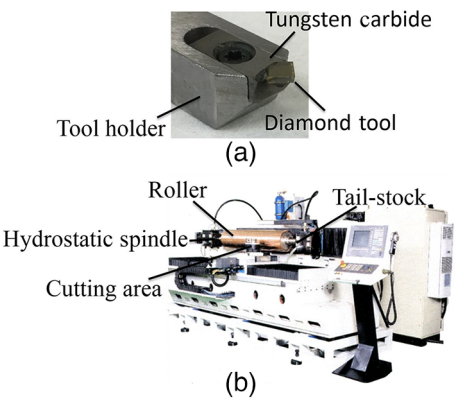

Fig. 3 (a) Single-point diamond tool and (b) Industrial Technology Research Institute drum roll lathe.

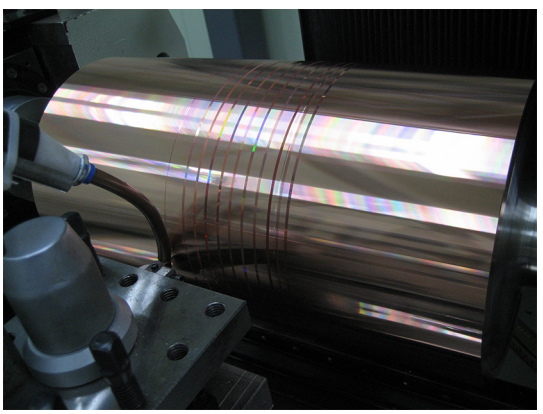

Fig. 4 Several molds with various periods and shapes on a roller for imprinting the subwavelength gratings.

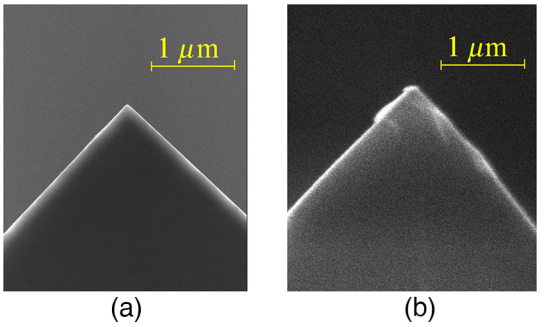

Fig. 5 SEM image of the diamond tool (a) before machining and (b) after machining.

The machining distance is around 30 km. As shown in Fig. 5(b), the tool wear is limited and the tool can still maintain its original shape after such a long-distance machining process. Therefore, the tool wear is not the major issue for the machinability of the molds in the cases studied.

Directly examining the molds machined on the drum roll shown in Fig. 4 was difficult. Therefore, the gratings fabricated using these molds were examined instead to evaluate the quality of the process. A UV resin was placed on a 188-μm-thick polyethylene terephthalate (PET) film, imprinted by the roller at a feed rate of 5 m/min, and then hardened with 100-W UV light (Fig. 6). An adequate imprinting pressure was applied to realize an acceptable replication rate ($\sim > 95\%$) for processing the designed gratings.[31]

Figures 7 and 8 show SEM images of subwavelength gratings with a lead angle of 45, 60, and 75 deg. As shown in Figs. 7(a) and 8(a), even when the molds were machined at a low-feed rate (equivalent to a low-grating period), the periods of the fabricated grating seemed to be consistent with one another when the mold machining process was conducted at a proper speed. However, when the molds were machined at a higher speed, the periods of the fabricated grating became irregular, as shown in Figs. 7(b) and 8(b). A comparison of the grating shown in Fig. 7(c) with those shown in Figs. 7(a) and 7(b) indicated that machining the molds at a higher feed rate (equivalent to a larger grating period) and a lower speed resulted in the formation of sharper edges; however, burrs occasionally formed at the top of the edges.

Figure 7(d) shows that the periods of the grating formed using molds machined at a higher speed were irregular, especially with the smallest period. The gratings formed using

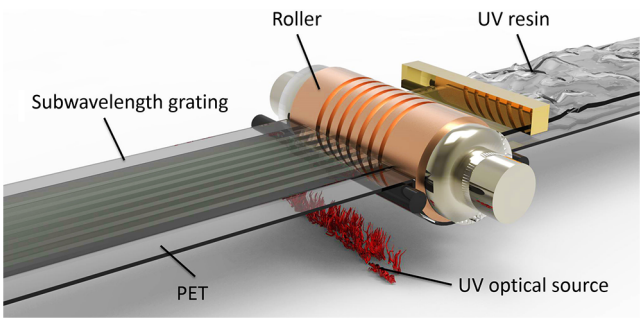

Fig. 6 UV resin was dispensed on the PET film, imprinted by the roller, and cured with a UV source.

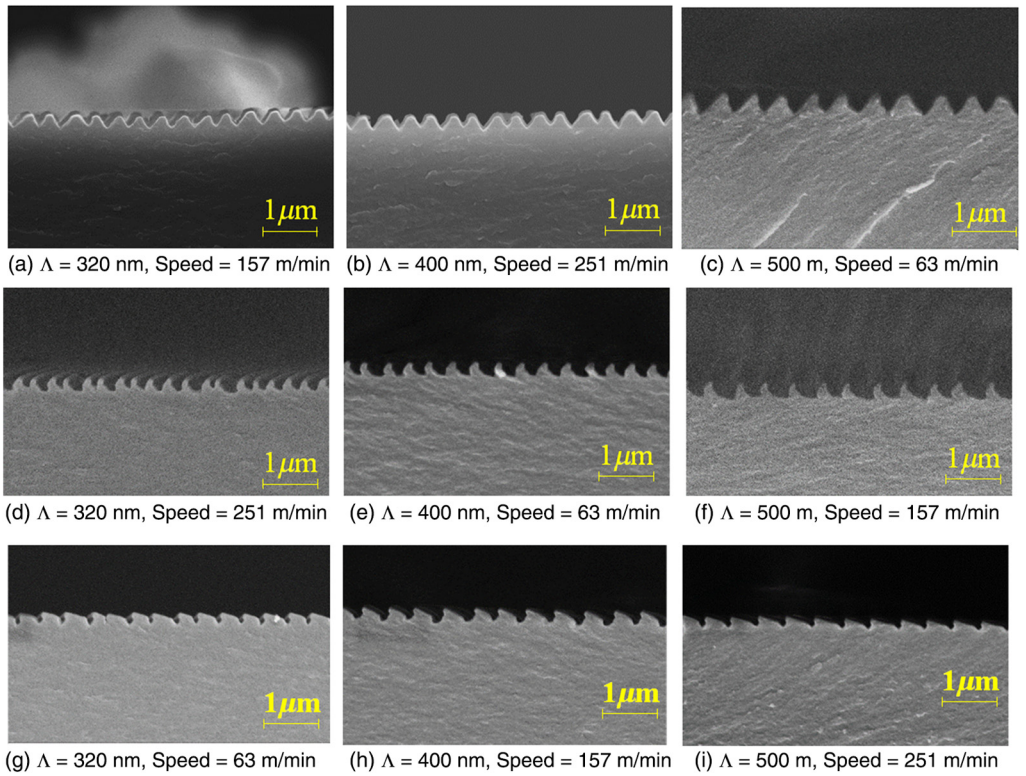

Fig. 7 SEM images: the cross section of subwavelength gratings with a lead angle of 45, 60, and 75 deg.

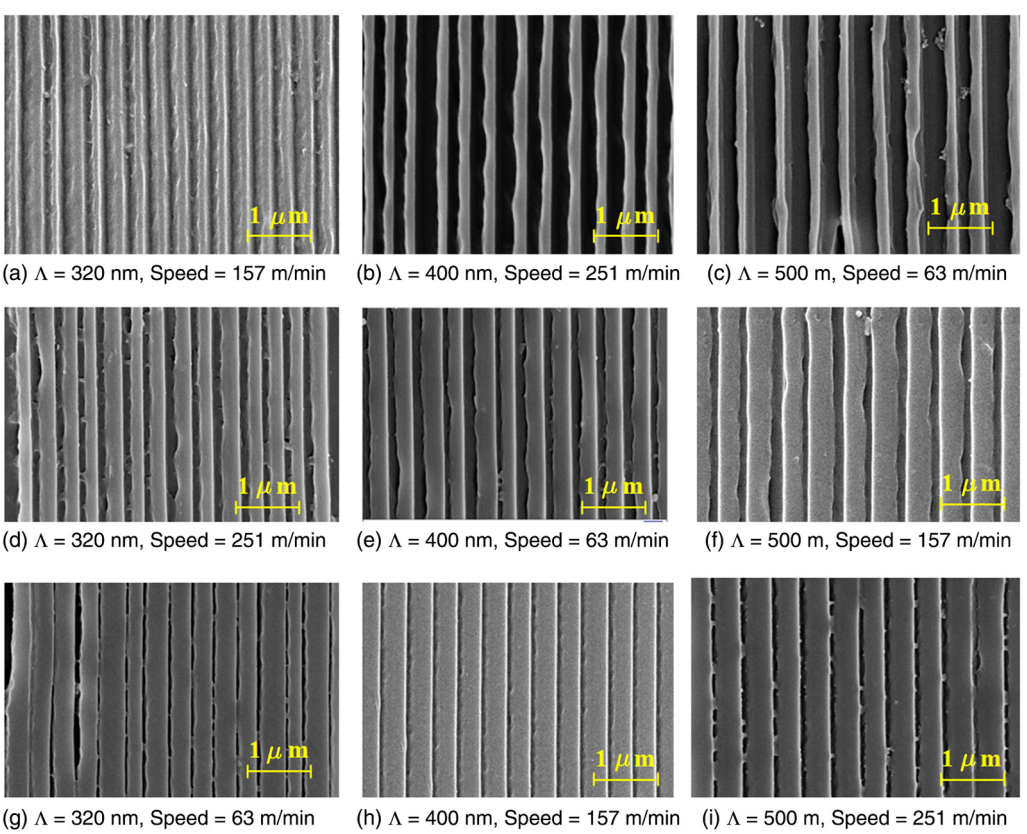

Fig. 8 SEM images: the top view of subwavelength gratings with a lead angle of 45, 60, and 75 deg.

molds machined at lower speeds had much regular periods, as shown in Figs. 7(e) and 7(f). However, overall, the shapes of the gratings seemed deformed. This deformation is possibly because of the demolding process, which entailed moving a mold from a grating in a perpendicular direction.

Notably, the periods of the grating fabricated using molds machined at the lowest speed were no longer consistent, as shown in Fig. 7(g). Moreover, all gratings shown in Figs. 7(g)–7(i) exhibited deformed shapes.

By examining all gratings shown in Figs. 7 and 8, the following observations were made:

1. Machining molds at the highest speed generally resulted in irregular grating periods. This might be due to vibrations that are readily engendered by high machining speeds.
2. Adequately determining the mold machining speed for fabricating gratings with small periods is critical for preventing the appearance of irregular periods.
3. The shapes of the gratings were frequently deformed, particularly when the shapes were asymmetric. The gratings with a lead angle of 45 deg demonstrated less shape deformations.
4. When the molds were machined at a higher feed rate and an appropriate speed, the values of grating periods were highly close to the desired values, with an error of 3% or lower.

4 Experiments for Grating Performance

The measurement module as shown in Fig. 9 was designed to evaluate the performance of the subwavelength gratings made. An emitted laser beam was incident to the prism horizontally. The wavelengths of three laser diodes were 633 nm (red), 532 nm (green), and 465 nm (blue). The incident angle to the grating was determined according to the direction of the rotator, as indexed by θ_{rot}. The relationship between the incident angle θ_{inc} and the prism rotation angle θ_{rot} was derived using Snell's law and the prism geometry. An $X-Y$ stage was used to move the laser vertically and to direct the laser beam to a specific grating area. Light propagating in the prism was extracted outwardly by the grating, and the spot pattern was measured by a power meter.

Figures 10–12 show a comparison of the normalized intensities of first-order transmission efficiency estimated

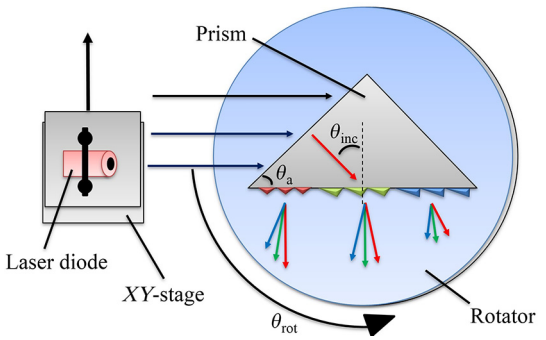

Fig. 9 Schematic of the measurement configuration.

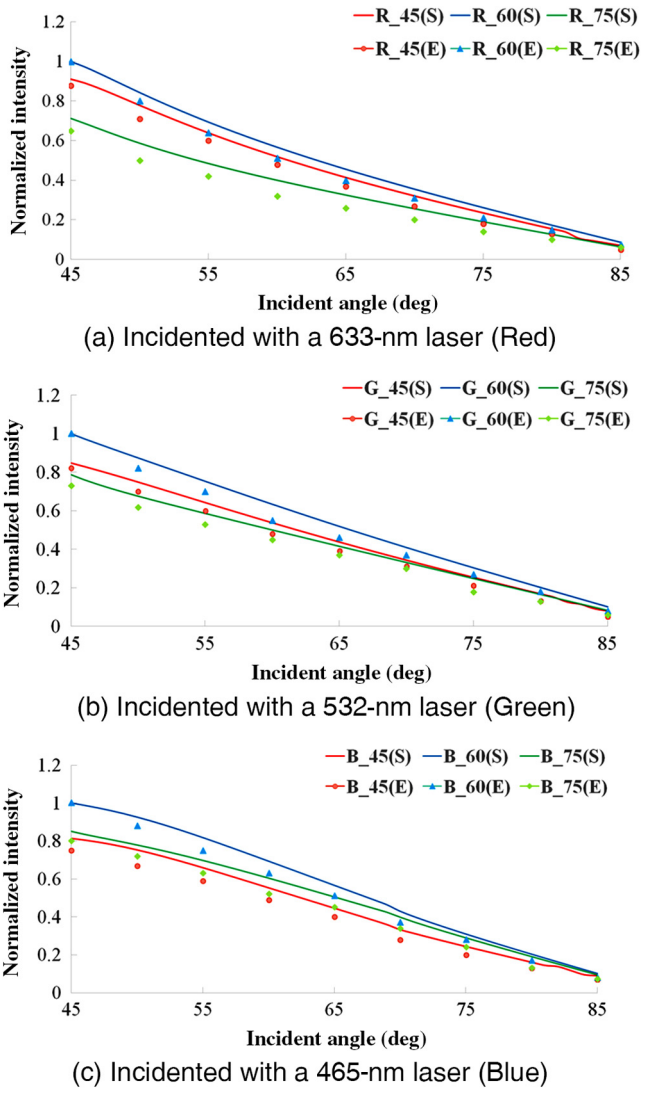

Fig. 10 Relationship between the normalized intensity and incident angle for grating with a period of 320 nm.

from the simulation results (S) and from measurement results (E) for the primary colors at various incident angles. According to these results, the following observations were made:

1. Inconsistencies were observed between the measurement results and simulation results. These inconsistencies may be partly due to the shape and height of the gratings formed being slightly different from those designed and used in the simulation.
2. Although the deformation occurred in the grating with a lead angle of 60 deg, the measurement results matched the simulation results well. This might be due to low-grating period variation and low-grating depth difference between peaks.
3. The DE and diffraction angle of gratings strongly depend on the value of the period and its shape.
4. As shown in Figs. 7(g)–7(i), the grating heights are smaller than the designed value due to the deformation when gratings with a lead angle of 75 deg were

fabricated. Therefore, the distributions of DEs are smaller than the simulation results.

5. As shown in Figs. 11(b) and 11(c), the performance of the grating with a lead angle of 60 deg was higher than that of the grating with a lead angle of 45 deg when a higher incident angle was applied. This might be because the grating with a lead angle of 45 deg exhibited an irregular shape when the mold was cut at the highest speed.
6. Compared with Figs. 10 and 11, the grating with a period of 500 nm has smaller errors than grating with a period of 320 and 400 nm, as shown in Fig. 12.

A diffractive module has been designed, fabricated, and tested. The main advantage of such a module is the convenience to detect the DE of grating. From the measurement of the subwavelength grating performance, the values matched the DEs by carefully controlling the precision of incident angles. For the consideration of uniformity and extracted energy, it is useful for the optical system such as displays, communication, and measurement.[1,10,11,13,27–29,31]

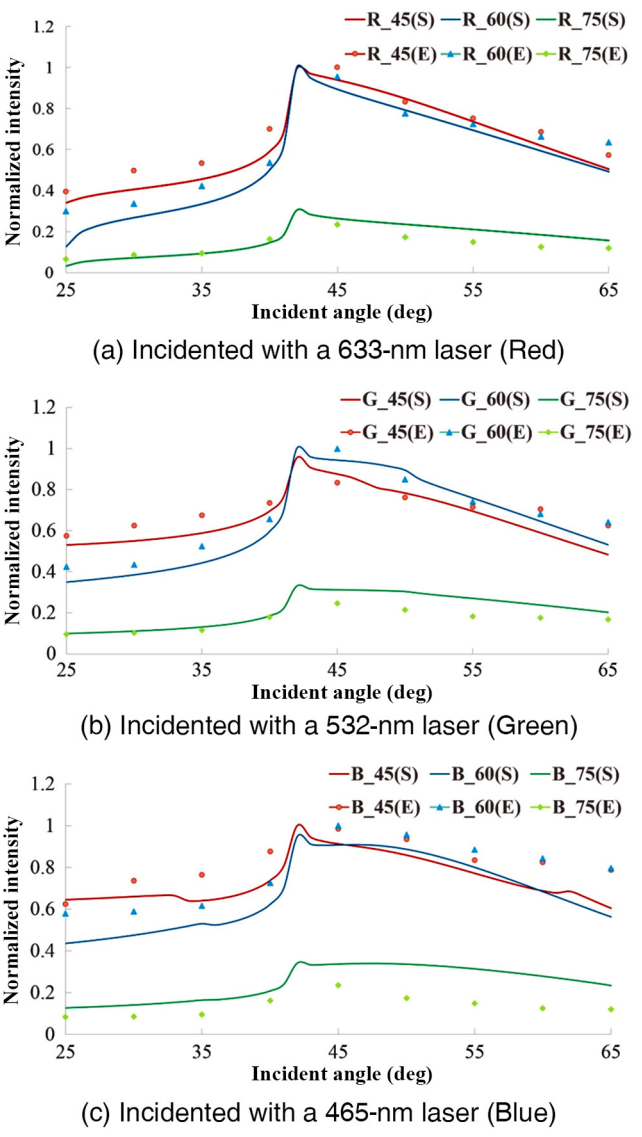

Fig. 11 Relationship between the normalized intensity and incident angle for grating with a period of 340 nm.

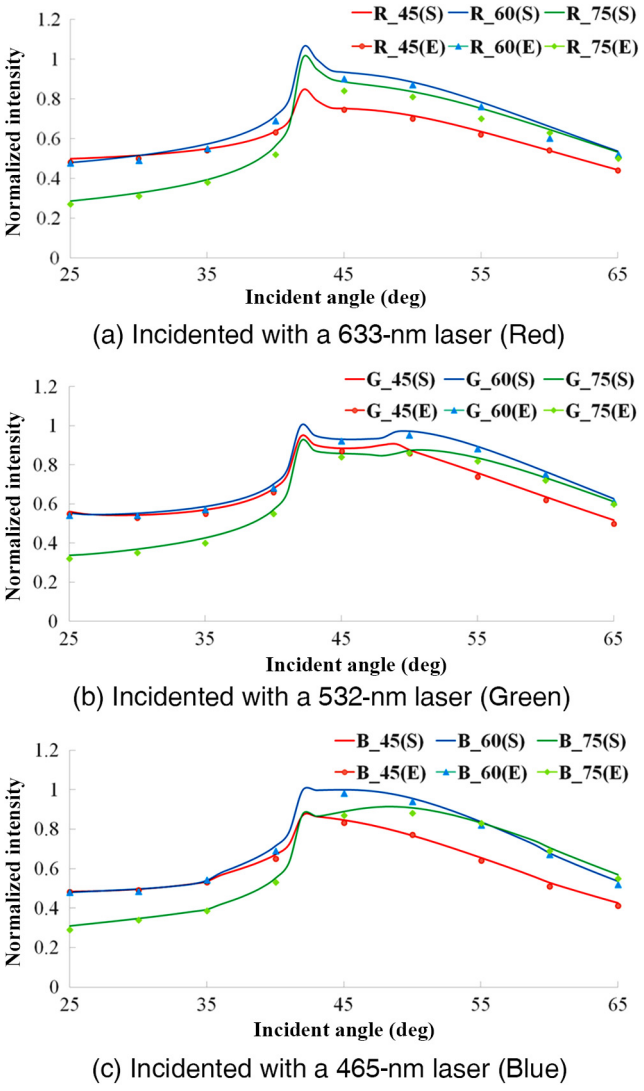

Fig. 12 Relationship between the normalized intensity and incident angle for grating with a period of 500 nm.

5 Conclusions

The DE of subwavelength gratings strongly depends on the periods and profiles of the grating microgrooves. In this study, the machinability of high-precision roll-to-roll imprinting molds was studied through diamond turning by using a single-point diamond cutting tool. Subwavelength gratings were fabricated through a roll-to-roll-based UV resin imprinting process executed using the fabricated molds. The results revealed that higher cutting speed was the most critical factor influencing the mold accuracy resulted in irregular grating periods. According to the optical measurement results, the performance of the subwavelength gratings adequately matched the design at various incident angles, particularly when a grating with a consistent grating period and shape was formed. This study demonstrates that through strict control of cutting parameters, diamond turning of high-precision molds is a feasible approach for ensuring the continual mass production of subwavelength gratings.

References

1. J. Kimmel, "Review paper: diffractive backlight technologies for mobile applications," *J. Soc. Inf. Display* **20**(5), 245–258 (2012).
2. S. R. Park et al., "Grating micro-dot patterned light guide plates for LED backlights," *Opt. Express* **15**(6), 2888–2899 (2007).
3. W. L. Barnes, A. Dereux, and T. W. Ebbesen, "Surface plasmon subwavelength optics," *Nature* **424**, 824–830 (2003).
4. Y. Kanamori, E. Roy, and Y. Chen, "Antireflection sub-wavelength gratings fabricated by spin-coating replication," *Microelectron. Eng.* **78–79**, 287–293 (2005).
5. C. Chevallier et al., "Optimized sub-wavelength grating mirror design for mid-infrared wavelength range," *Appl. Phys. A* **103**(4), 1139–1144 (2011).
6. G. Zhou et al., "High-speed, high-optical-efficiency laser scanning using a MEMS-based in-plane vibratory sub-wavelength diffraction grating," *J. Micromech. Microeng.* **18**(8), 134–144 (2008).
7. H. Lochbihler, "Colored images generated by metallic sub-wavelength gratings," *Opt. Express* **17**(14), 12189–12196 (2009).
8. H. Subbaraman et al., "Efficient light coupling into in-plane semiconductor nanomembrane photonic devices utilizing a sub-wavelength grating coupler," *Opt. Express* **20**(18), 20659–20665 (2012).
9. P. J. Bock et al., "Demultiplexer with blazed waveguide sidewall grating and sub-wavelength grating structure," *Opt. Express* **16**(22), 17616–17625 (2008).
10. D. Donisi, R. Caputo, and G. Cennini, "Holographic grating based high sensitivity device for refractive index measurements," *Opt. Express* **18**(14), 15236–15241 (2010).
11. R. Caputo et al., "Short period holographic structures for backlight display applications," *Opt. Express* **15**(17), 10540–10552 (2007).
12. L. Ye et al., "All-nanoparticle concave diffraction grating fabricated by self-assembly onto magnetically-recorded templates," *Opt. Express* **21**(1), 1066–1075 (2013).
13. F. Pastorelli et al., "Self-assembled plasmonic oligomers for organic photovoltaics," *Adv. Opt. Mater.* **2**(2), 171–175 (2014).
14. H. Tan, A. Gilbertson, and S. Y. Chou, "Roller nanoimprint lithography," *J. Vac. Sci. Technol. B* **16**, 3926–3928 (1998).
15. T. Mäkelä et al., "Continuous roll to roll nanoimprinting of inherently conducting polyaniline," *Microelectron. Eng.* **84**(5–8), 877–879 (2007).
16. T. Mäkelä et al., "Utilizing roll-to-roll techniques for manufacturing source-drain electrodes for all-polymer field-effect transistors," *Synth. Met.* **153**(1–3), 285–288 (2005).
17. F. Pastorelli et al., "The organic power transistor: roll-to-roll manufacture, thermal behavior, and power handling when driving printed electronics," *Adv. Eng. Mater.* **18**(1), 51–55 (2016).
18. V. W. Jones et al., "Roll to roll manufacturing of subwavelength optics," *Proc. SPIE* **7205**, 720501 (2009).
19. H. Hocheng and M. L. Hsieh, "Signal analysis of surface roughness in diamond turning of lens molds," *Int. J. Mach. Tools Manuf.* **44**(15), 1607–1618 (2004).
20. H. Hocheng et al., "A brighter place: overview of microstructured sunlight guide," *J. Achiev. Mater. Manuf. Eng.* **43**(1), 409–417 (2010).
21. K. F. Zhang and L. Kun, "Classification of size effects and similarity evaluating method in micro forming," *J. Mater. Process. Technol.* **209**(11), 4949–4953 (2009).
22. N. Ikawa, S. Shimada, and H. Tanaka, "Minimum thickness of cut in micromachining," *Nanotechnology* **3**(1), 6–9 (1992).
23. J. D. Drescher and T. A. Dow, "Tool force model development for diamond turning," *Precis. Eng.* **12**(1), 29–35 (1990).
24. K. Sawada et al., "Development of ultraprecision micro grooving: manufacture of V-shaped groove," *JSME Int J. Ser. C* **43**(1), 170–176 (2000).
25. M. G. Moharam, E. B. Grann, and D. A. Pommet, "Formulation for stable and efficient implementation of the rigorous coupled-wave analysis of binary gratings," *J. Opt. Soc. Am. A* **12**(5), 1068–1076 (1995).
26. X. H. Rao et al., "Study on the zero order reflection efficiency of sub-wavelength grating," *J. Univ. Shanghai Sci. Technol.* **29**(3), 245–249 (2007).
27. C.-W. Liu et al., "Roll-to-roll process-based sub-wavelength grating for a color-separation backlight," *IEEE/OSA J. Disp. Technol.* **9**(7), 561–564 (2013).
28. S. M. Lee et al., "New concept for improvement of white color balance in hologram back-light units," in *SID Symp. Digest of Technical Papers (SID '03)*, Vol. 49, pp. 1361–1363, Wiley, (2003).
29. C.-W. Liu, C.-C. Wu, and S.-C. Lin, "A simple and wide-range refractive index measuring approach by using a sub-micron grating," *Appl. Phys. Lett.* **106**, 151907 (2015).
30. E. Miyamoto et al., "Novel diffraction grating light guide for LED backlight," *Proc. SPIE* **6488**, 64880H (2007).
31. C. W. Liu et al., "Submicrometer grating light bar for a color-separation backlight," *Appl. Opt.* **52**(15), 3617–3623 (2013).

Chun-Wei Liu received his MS degree in power mechanical engineering from National Tsing Hua University, Taiwan, in 2010, where he is currently pursuing his PhD in the Department of Power Mechanical Engineering, National Tsing Hua University. His recent research interest is optical structure design based on the roll-to-roll ultraprecision process.

Jiwang Yang received his PhD degree from Tohoku University in 2000. He is a professor with Faculty of Science and Technology, Keio University, Japan. His current research interests include production engineering/processing studies, material processing/treatment, micro/nanodevice, applied physical properties/crystal engineering.

Shih-Chieh Lin received the BS degree in mechanical engineering from National Taiwan University, Taiwan, the MS and PhD degree in mechanical and industrial engineering from University of Illinois at Urbana-Champaign in 1989. He is a professor with the Department of Power Mechanical Engineering, Naional Tsing Hua University in Taiwan. His current research interests include manufacturing process modeling and monitoring, instrument developing, optical component design, metrology, and tribology.